Influence of Tempering on the Microstructure and Mechanical Properties of HSLA-100 Steel Plates

S.K. DHUA, D. MUKERJEE, and D.S. SARMA

The influence of tempering on the microstructure and mechanical properties of HSLA-100 steel (with C-0.04, Mn-0.87, Cu-1.77, Cr-0.58, Mo-0.57, Ni-3.54, and Nb-.038 pct) has been studied. The plate samples were tempered from 300 °C to 700 °C for 1 hour after austenitizing and water quenching. The transmission electron microscopy (TEM) studies of the as-quenched steel revealed a predominantly lath martensite structure along with fine precipitates of Cu and Nb(C, N). A very small amount of retained austenite could be seen in the lath boundaries in the quenched condition. Profuse precipitation of Cu could be noticed on tempering at 450 °C, which enhanced the strength of the steel significantly (yield strength (YS)—1168 MPa, and ultimate tensile strength (UTS)—1219 MPa), though at the cost of its notch toughness, which dropped to 37 and 14 J at 25 °C and −85 °C, respectively. The precipitates became considerably coarsened and elongated on tempering at 650 °C, resulting in a phenomenal rise in impact toughness (Charpy V-notch (CVN) of 196 and 149 J, respectively, at 25 °C and −85 °C) at the expense of YS and UTS. The best combination of strength and toughness has been obtained on tempering at 600 °C for 1 hour (YS-1015 MPa and UTS-1068 MPa, with 88 J at −85 °C).

I. INTRODUCTION

STEELS used for high-strength structural applications are essentially quenched and tempered low- to medium-carbon low-alloy steels. In the United States Navy's specification, these are basically HY series of steels that are primarily low-alloy Ni-Cr-Mo-V steel with about 0.2 pct C (Tables I and II). The HY series of steels has been most commonly used for submarine hulls for over 4 decades.[1] In this series of steels, the initial development of the HY-80 was followed by the HY-100 and the HY-130 steels (the number indicates yield strength (YS) in Ksi; 1 Ksi = 7 MPa). Carbon is the main martensitic strengthening element in these steels; with a carbon equivalent of around 0.80, the steels are difficult to weld and require costly preheating as well as postweld heat treatments.[2,3] To overcome these difficulties, a new family of low-carbon, copper-bearing, high-strength, low-alloy steels has been developed during the last 2 decades (Tables I and II). These steels are intended for use in the construction of the hulls of naval warships and submarines and also for engineering structures, especially mining and dredging equipment, offshore drilling platforms, heavy duty trucks, and bridges, *etc.*[1,3–5] Using high strength, good impact toughness, and easy weldability as the major criteria, low-alloy steels with a very low carbon content (<0.06 pct) and a combination of alloying elements (Cu, Ni, Cr, Mo, Nb, and V) were developed. Copper was added primarily to cause precipitation hardening. The first successful development in this family of steels was an ASTM A 710 grade with a composition 0.07 pct C, 0.5 pct Mn, 0.4 pct Si, 0.75 pct Cr, 0.9 pct Ni, 0.20 pct Mo, 1.15 pct Cu, and 0.02 pct Nb for use in offshore structures.[6–11] Based on this, HSLA-80 steel was developed by the United States Navy in the early 1980s.[1,12] Thomson *et al.* worked with a similar HSLA steel with a higher alloy modification.[13] More recently, they worked in detail on the austenite decomposition during continuous cooling on an HSLA-80 plate steel.[14] Although HSLA-80 steel has a minimum YS of 80 Ksi (552 MPa) with a good low-temperature impact toughness (81 J at −85 °C) and weldability, there was a need to develop steels with a still higher YS for making many critical components of naval and engineering structures that were subjected to complex dynamic loading.[1] With this in mind, a few United States steel companies (Lukens Steel, Coatesville, Pennsylvania, Phoenix Steel Corporation, Claymont, Delaware, *etc.*) and the United States Navy have concentrated on the development of HSLA-100 steel with a minimum YS of 100 Ksi (690 MPa) with a low-temperature impact toughness (81 J at −85 °C) and easy weldability. A few trial heats were made with these steels in the late 1980s and early 1990s. Wilson *et al.*[3] worked with two such HSLA-100 steels, of 28-mm plate thickness with carbon contents of 0.04 wt pct and 0.06 wt pct, and found that the plate with the slightly higher carbon content (0.06 wt pct) gave better strength than the plate with the lower carbon content (0.04 wt pct). Fox *et al.*[15] worked on HSLA-100 steels of 19- and 32-mm plate thickness with normal copper (1.47 wt pct) as well as with increased copper (2.0 wt pct). For the same section thickness, the higher copper content gave better strength and toughness.[15] Mujahid *et al.*,[4,16] on the other hand, worked with 25-mm plates of HSLA-100 steels with carbon contents of 0.036 pct and 0.057 pct. They attributed the extraordinary improvement in toughness that they observed when the steels were aged between 640 °C and 665 °C to the "new austenite" formed at the martensite lath boundaries.

The present investigation is mainly aimed at a study of the evolution of the microstructure of the HSLA-100 steel that occurs on tempering and its effect on the steel's mechanical properties.

S.K. DHUA, Principal Research Manager, and D. MUKERJEE, Deputy General Manager, are with the Research and Development Centre for Iron and Steel, Steel Authority of India Limited, Ranchi - 834 002, India. D.S. SARMA, Professor, is with the Department of Metallurgical Engineering, Banaras Hindu University, Varanasi - 221 005, India.

Manuscript submitted May 16, 2000.

Table I. Specified Chemical Composition of HSLA Steels Used for Naval Ship Building and Off-Shore Structures (Composition in Weight Percent, Maximum Unless a Range is Shown)

Steels Grade	Specification/ Year of Introduction	C	Mn	P	S	Si	Ni	Cr	Mo	Cu	V	Ti	Nb
HY-80	MIL-S-16216K (1950s)	0.13 to 0.18	0.1 to 0.4	0.015	0.008	0.15 to 0.38	2.5 to 3.5	1.4 to 1.8	0.35 to 0.6	0.25	0.03	0.02	—
HY-100	MIL-S-16216K (1960s)	0.14 to 0.2	0.1 to 0.4	0.015	0.008	0.15 to 0.38	2.75 to 3.5	1.4 to 1.8	0.35 to 0.6	0.25	0.03	0.02	—
HY-130	MIL-S-24371 (1960s)	0.12	0.6 to 0.9	0.01	0.008	0.15 to 0.35	4.75 to 5.25	0.4 to 0.7	0.3 to 0.65	0.25	0.05 to 0.1	0.02	0.02
A 710	ASTM A 710 Gr-A, Cl-III (1977)	0.07	0.4 to 0.7	0.025	0.025	0.4	0.7 to 1.0	0.6 to 0.9	0.15 to 0.25	1 to 1.3	—	—	0.02
HSLA-80	MIL-S-24645A (1984)	0.06	0.4 to 0.7	0.02	0.006	0.4	0.7 to 1.0	0.6 to 0.9	0.15 to 0.25	1 to 1.3	0.03	0.02	0.02 to 0.06
HSLA-100	MIL-S-24645A (1989)	0.06	0.75 to 1.15	0.02	0.006	0.4	3.35 to 3.65	0.45 to 0.75	0.55 to 0.65	1.45 to 1.75	0.03	0.02	0.02 to 0.06

II. EXPERIMENTAL

The steel was supplied by the Phoenix Steel Corporation (Claymont, Delaware) in the form of austenitized and quenched plates of a 51-mm thickness from a 150-ton trial production heat. The chemical analysis of the steel was conducted by optical emission spectrometry; the composition is provided in Table III. To evaluate the mechanical properties (hardness, Charpy impact toughness, and tensile strength) of the steel at various tempering conditions, 14-mm-thick Charpy impact specimens and tensile test blocks of suitable length and width in the longitudinal transverse (L-T) orientation were cut from the as-received plate. To maintain the uniformity of sample location, the test blocks were cut at a distance of 2 to 3 mm from the top and bottom surfaces. The test blocks were then austenitized at 950 °C for 40 minutes in a salt bath furnace, and quenched in water. They were then tempered at temperatures varying from 300 °C to 700 °C at intervals of 50 °C for 1 hour in the same furnace, followed by water quenching.

After tempering, the samples were machined to final dimensions. Shouldered tensile specimens of a 25-mm gage length and a 6.25-mm gage diameter (per ASTM A 370) were used in the present investigation. Tensile testing was carried out with an Instron 1195 (Instron Ltd., High Wycombe, Buckinghamshire, England) universal testing machine at a crosshead speed of 1 mm/min. Standard Charpy samples, with dimensions of 10 × 10 × 55 mm and a 2-mm V-notch, were prepared according to ASTM E 23. Impact tests were conducted with a Tinius-Olsen model Charpy impact testing machine at various temperatures, namely room temperature (25 °C), −20 °C, and −85 °C. For both tensile and impact testing, three specimens were tested for each condition, and average values were reported. The hardness was measured in a Vicker's hardness tester (Georg Reicherter, Esslingen/Neckar, Germany) using a 30-kg load. An average hardness of 10 indented fields for a particular sample was reported. The error in hardness measurement was ±5 Vickers hardness numbers (VHN), while the error in the cases of YS and ultimate tensile strength (UTS) was ±10 MPa. The error in measurement of the percent of elongation (EL) and the percent of reduction in area (RA) was ±1 pct, whereas it was ±5 Charpy V-notches (CVN), in the case of CVN values.

Fractography studies were carried out on the tested impact specimens in a JSM-840A model scanning electron microscope (SEM) (JEOL Ltd., Tokyo, Japan). X-ray diffractometric (XRD) studies of the as-quenched and tempered steels were conducted to detect the presence of retained austenite, using a Siemens X-ray diffractometer (Siemans, Karl Sruhe, Germany), with a Mo K_α target.

Light microscopy studies were conducted on the samples taken from the tested Charpy samples at similar locations. Samples were mechanically polished and etched with a 2 pct nital solution for observation of the microstructure using a Neophot-30 optical microscope (Carl Zeiss, Jena, Germany). For the measurement of grain size, hot-stage microscopy was done at 950 °C using a Reichert MeF_2 light microscope with vacuutherm (Leica, Wetzlar, Germany), with a 7-mm diameter cylindrical solid specimen 10 mm in length. Thin foils were prepared for transmission electron microscopy (TEM) in a twin jet electropolisher, using a solution of 95 pct glacial acetic acid and 5 pct perchloric

Table II. Specified Mechanical Properties of HSLA Steels Used for Naval Ship Building and Off-Shore Structures

Steel Grade	YS (MPa)	El Percent	RA Percent	Charpy Impact Energy (J)		
				−17.7 °C	−60 °C	−84.4 °C
HY-80	552 to 687	20	50	81	—	47
HY-100	690 to 828	18	45	81	—	54
HY-130	897 to 1035	15	50	108	—	54
ASTM A 710, Gr.-A, Cl.-III	345 to 585	—	—	—	69	—
HSLA-80	552 to 690	20	50	—	—	81
HSLA-100	690 to 862	18	45	108	—	81

Table III. Chemical Composition of the Experimental Steel (Weight Percent)

C	Mn	P	S	Si	Cu	Ni	Cr	Mo	Al	Nb
0.04	0.87	0.003	0.006	0.25	1.77	3.54	0.58	0.57	0.038	0.038

acid at 10 °C and 25 V. The foils were examined in a JEOL*

*JEOL is a trademark of Japan Electron Optics, Ltd., Tokyo.

4000 EX microscope at 200 kV. Energy-dispersive spectrometry (EDS) of a few thin foils was conducted with a Link EDS system (Oxford Instruments Ltd., High Wycombe, Buckinghamshire, England).

III. RESULTS

A. *Microstructure*

1. *Light microscopy*

Typical optical micrographs of the as-quenched steel and the steel tempered at 700 °C are shown in Figures 1(a) and (b), respectively. These micrographs do not reveal much other than that the as-quenched steel exhibited a lath martensite microstructure and that it did not undergo any marked changes on tempering at 700 °C. The prior austenite grain size of the steel measured by hot-stage microscopy was found to be 15 μm.

2. *Transmission electron microscopy*

The TEM studies of the as-quenched steel revealed a predominantly lath martensite structure with a high dislocation density (Figure 2(a)). Extremely fine precipitates about 10 to 15 nm in diameter could also be seen in the dark-field (DF) micrograph of Figure 2(b). The selected area diffraction (SAD) pattern shown in Figure 2(c) and its sketch, Figure 2(d), indicated that the precipitates were essentially Nb(C, N) and Cu. The DF image shown in Figure 2(b) essentially corresponded to a (111) Cu ring. Since a (111) Nb(C, N) ring was located close to the (111) Cu ring, the appearance of some of the Nb(C, N) precipitates in that DF image could not be ruled out. Traces of retained austenite were observed at very few lath boundary locations in the as-quenched condition; it was identified by SAD, as shown in Figure 2(e) and its sketch, Figure 2(f). The DF image from the (022) austenite reflection is shown in Figure 2(g), which is taken from a different area than Figures 2(a) to (d).

The TEM studies of the steel tempered at 350 °C and 400 °C showed a microstructure similar to the one found in the as-quenched steel. The number of Cu precipitates has considerably increased on tempering at 450 °C, as can be seen in the bright-field (BF) and DF micrographs of Figures 3(a) and (b). The Cu precipitates, however, did not coarsen much at this temperature, and these were only slightly coarsened to ~20-nm diameter after tempering at 600 °C, as shown in Figure 4. Extremely fine spherical Nb(C, N) particles were found along with Cu precipitates in all tempering conditions. Thus, the BF images shown in Figures 3(a) and 4 also indicated the presence of Nb(C, N) precipitates along with the Cu precipitates. The DF image shown in Figure 3(b) was essentially from the (111) Cu ring and, as mentioned earlier, some of the DF spots might correspond to the closely located (111) Nb(C, N) ring.

The steel tempered at 650 °C continued to exhibit martensite laths. The martensite freshly formed from the intercritical

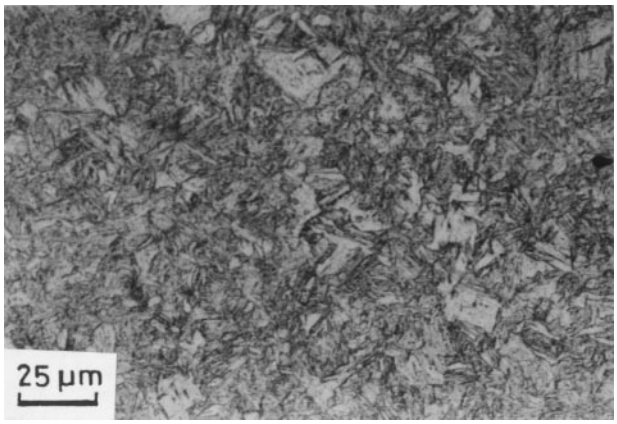

(*a*)

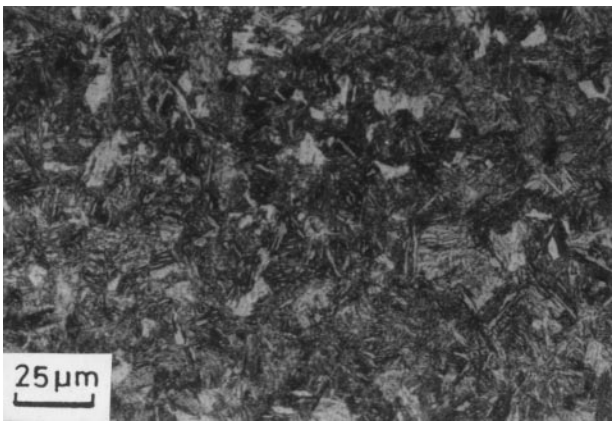

(*b*)

Fig. 1—Optical microstructures of the steel (*a*) water-quenched and (*b*) tempered at 700 °C.

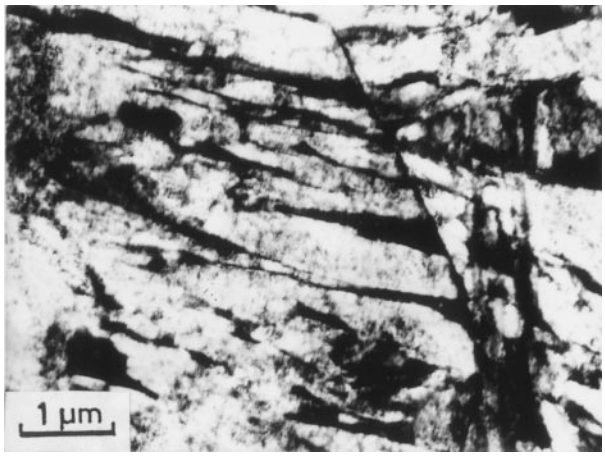

(*a*)

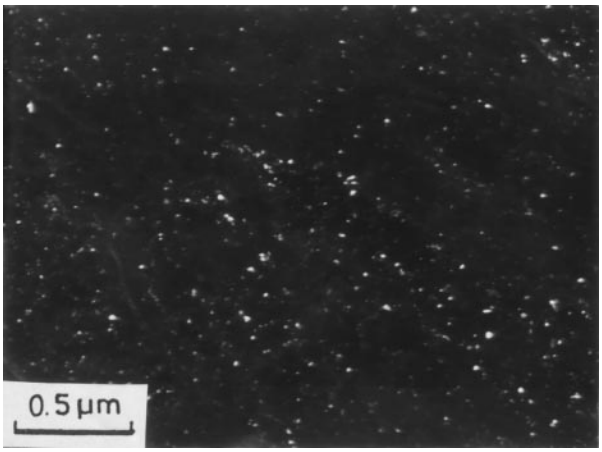

(*b*)

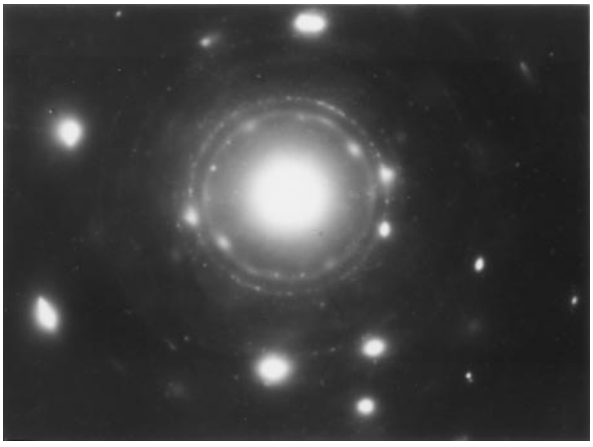

(*c*)

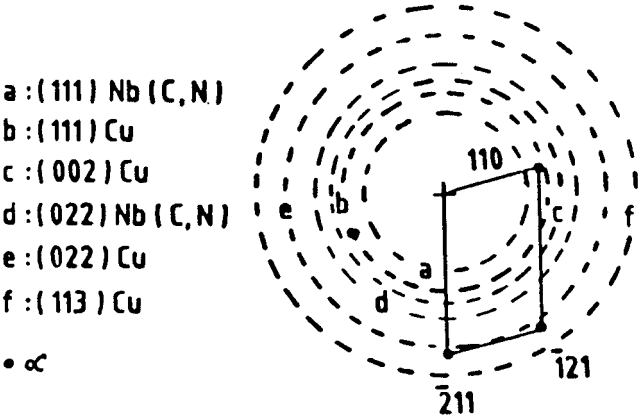

(*d*)

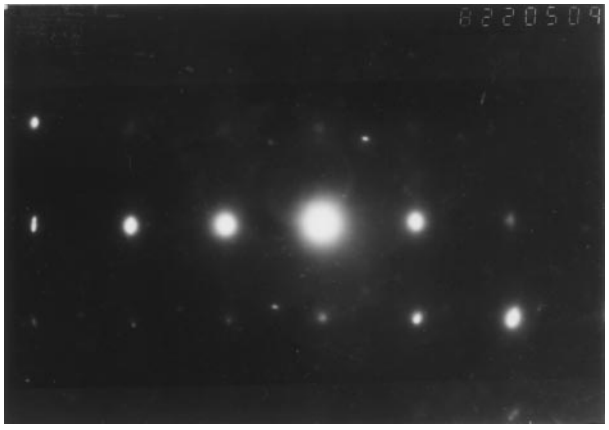

(*e*)

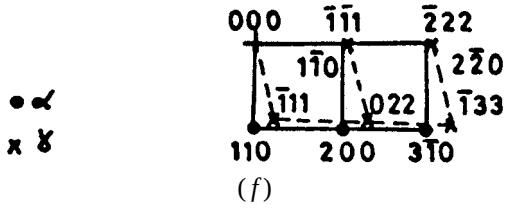

(*f*)

Fig. 2—TEMs of the steel in water-quenched condition: (*a*) BF revealing lath martensite; (*b*) DF; (*c*) SAD; and (*d*) schematic of SAD, identifying the Nb(C, N) and Cu precipitates. (*e*) SAD and (*f*) schematic of SAD showing α and γ reflections.

austenite could also be seen as a dark phase at the lath boundaries (Figure 5(a)). Precipitates were found within the laths as well as at the lath boundaries. The diffraction analyses of the lath boundary phase revealed that it was essentially a bcc phase, and that it could be either ferrite or martensite but not austenite. The Cu precipitates have become bigger and rod-shaped (50-nm long) at this temperature, the evidence of which is shown in BF and DF images (Figures 5(b) and (c)). Few Nb(C, N) precipitates were also present in the structure. Since the Nb(C, N) precipitates were inherited from the austenite structure, and were not expected to grow on tempering, some of the fine and spherical particles observed in the BF and DF images shown in Figures 5(b) and (c) could be of Nb(C, N). The SAD pattern and its sketch taken from the same field are exhibited in Figures 5(d) and (e), which confirmed the presence of both Cu and Nb(C, N) rings. The DF image shown in Figure 5(c) essentially corresponded to the (111) Cu ring and was ex-

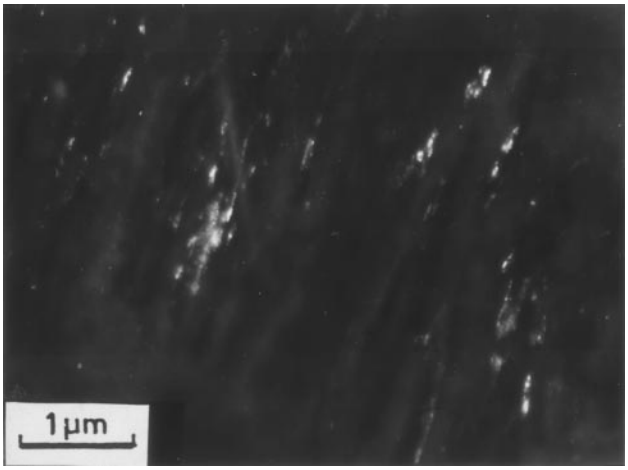

(*g*)

Fig. 2—Continued. TEMs of the steel in water-quenched condition: (*g*) DF with (022) γ reflection revealing retained austenite at lath boundaries.

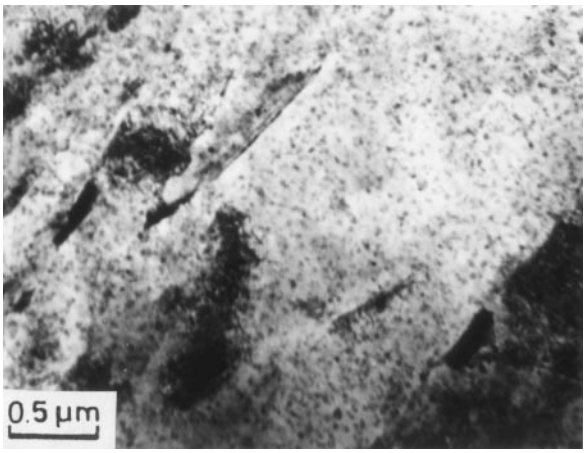

(*a*)

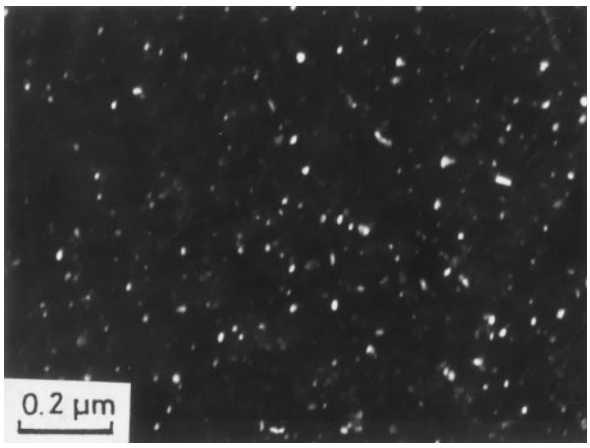

(*b*)

Fig. 3—TEMs of the steel tempered at 450 °C depicting profuse precipitation of Cu throughout the matrix with a few Nb(C, N) precipitates: (*a*) BF and (*b*) DF.

pected to have some area from the (111) Nb(C, N) ring located close to it.

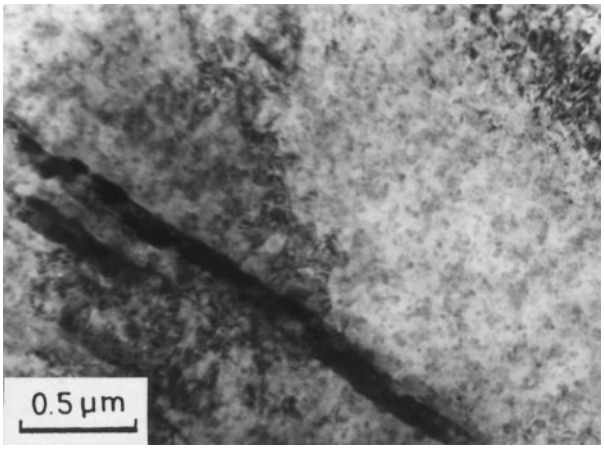

Fig. 4—TEM of the steel tempered at 600 °C revealing unrecovered martensite laths and large numbers of Cu with a few Nb(C, N) precipitates within its matrix.

After 700 °C tempering, the volume percent of the new lath boundary phase was found to be greater (Figure 6(a)). The Cu precipitates were coarse and rod-shaped, though fewer in number at this temperature (Figure 6(b)). Two superimposed EDS spectra of the lath boundary dark phase and the adjacent matrix are shown in Figure 6(c). The quantitative analyses revealed an approximately 50 pct enrichment of Mn and 35 pct enrichment of Ni in the former, as compared to the adjacent matrix.

B. *Mechanical Properties*

The hardness of the quenched steel as a function of tempering temperature is plotted in Figure 7, which indicates that the VHN increased from 354 in the as-quenched condition to a high of 388 after tempering at 450 °C, beyond which it decreased to a low of 289 after tempering at 650 °C. A slight increase in hardness to 309 VHN was noticed in the steel after tempering at 700 °C.

The variations in the YS and UTS of the steel with tempering temperature are also depicted in Figure 7. The YS varied within a range of 806 to 1168 MPa. The YS was highest after tempering at 450 °C and lowest after 700 °C tempering. The UTS also varied more or less in the same fashion, increasing from 1134 to 1219 MPa at 450 °C, before falling to 938 MPa after 650 °C tempering. A slight increase in UTS to 1041 MPa was observed in the steel after tempering at 700 °C.

The variations of EL percent and RA percent with tempering temperature are plotted in Figure 8. The EL percent varied between 17 and 23. The maximum EL was achieved after tempering at 650 °C, and the minimum was achieved at 300 °C to 350 °C. The RA percent varied from 59 to 73. The maximum RA was obtained after tempering at 650 °C, and the minimum was observed after tempering at 450 °C.

The CVN impact energies of the quenched and tempered steels were measured at room temperature (25 °C), −20 °C and −85 °C. The highest CVN energies at room temperature, −20 °C and −85 °C were 196, 190, and 149 J, respectively, which were obtained in samples tempered at 650 °C. The lowest CVN energies at room temperature, −20 °C, and −85 °C were 37, 19, and 14 J, respectively, which were obtained in samples tempered at 450 °C. Figure 9 depicts

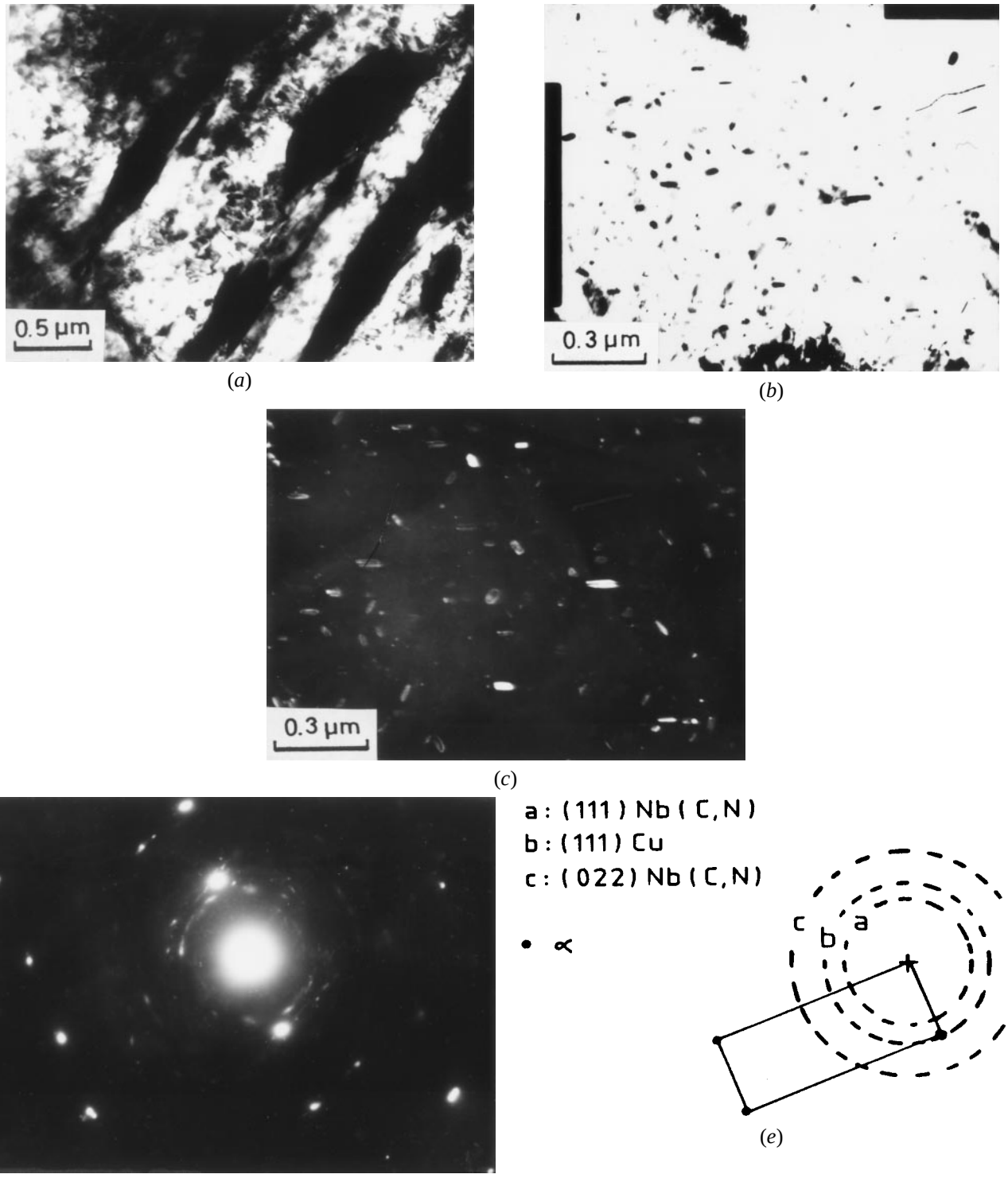

Fig. 5—TEMs of the steel tempered at 650 °C depicting (*a*) partially recovered matrix with freshly formed martensite appearing as dark phase at lath boundaries. (*b*) BF and (*c*) DF showing elongated and rod-shaped Cu precipitates with a few fine and spherical Nb(C, N) precipitates. (*d*) SAD and (*e*) schematic of SAD, identifying Cu and Nb(C, N) precipitates.

the variation in CVN energies with tempering temperature at various test temperatures.

C. *Fractography*

Fractographic studies of the tested impact samples of the as-quenched and tempered steels were made through SEM. Figures 10(a) through (c) show the typical fractographs of broken Charpy samples tested at −85 °C, from as-quenched steel and from steel tempered at 450 °C and 650 °C, respectively. While the samples belonging to the as-quenched steel and the steel tempered at 650 °C exhibited dimples, the fracture surfaces of the steel tempered at 450 °C were quasi-cleavage consistent with the poor notch toughness of the steel in this condition.

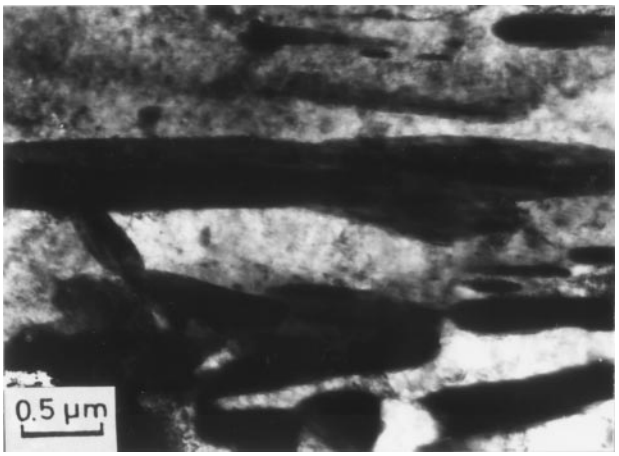

(*a*)

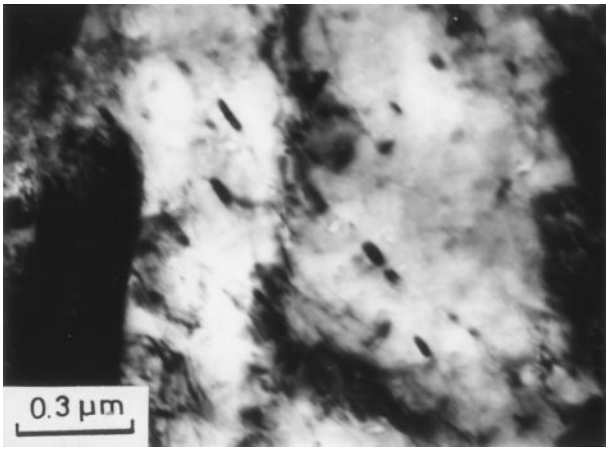

(*b*)

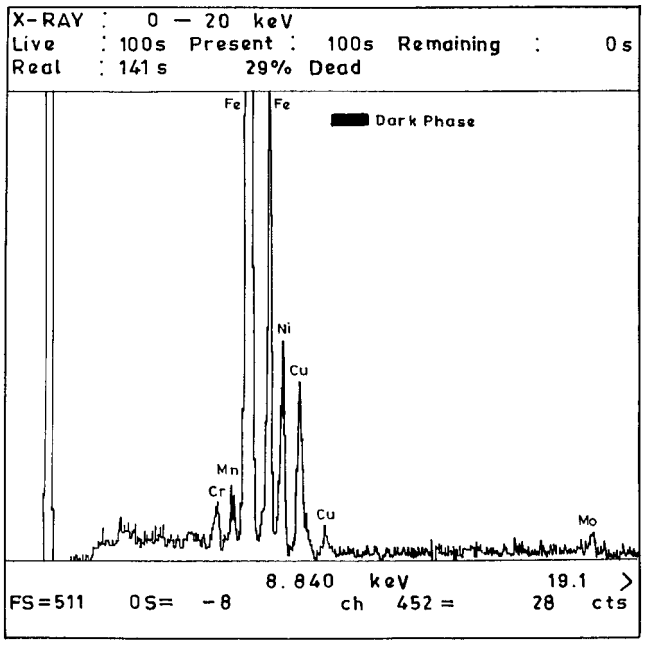

(*c*)

Fig. 6—TEMs of the steel tempered at 700 °C revealing (*a*) partially recovered matrix with a large quantity of freshly formed martensite (dark phase). (*b*) Elongated Cu precipitates. (*c*) Two superimposed EDS spectra from the dark phase and adjacent matrix confirming enrichment of Mn and Ni in the former.

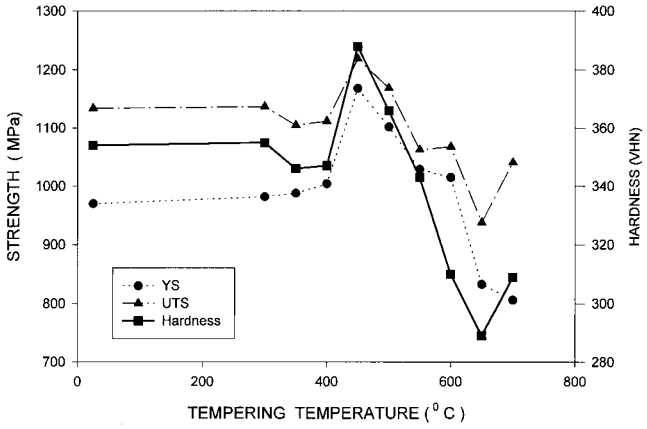

Fig. 7—Variation of YS, UTS, and VHN of the steel with tempering temperature.

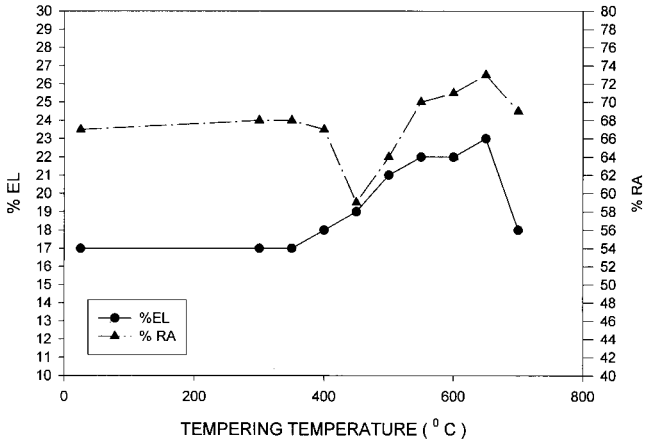

Fig. 8—Variation of EL percent and RA percent of the steel with tempering temperature.

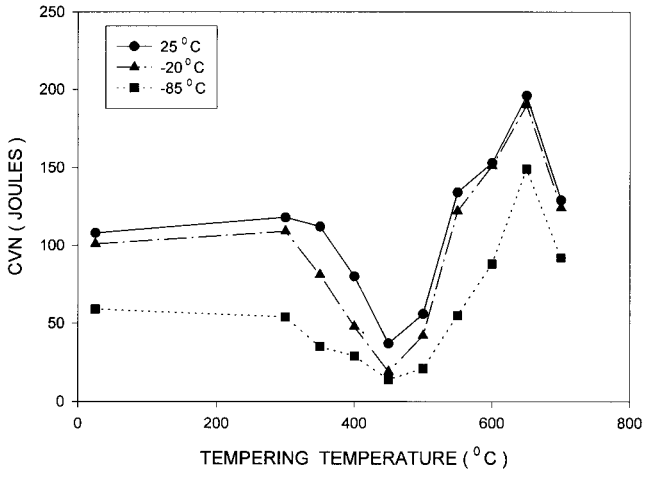

Fig. 9—Variation of CVN of the steel at 25 °C, −20 °C, and −85 °C with tempering temperature.

D. *X-Ray Diffractometry*

The XRD studies conducted on the water-quenched and tempered steels did not reveal the presence of retained austenite in any condition. This implies that the amount of retained austenite is much less than 2 pct.

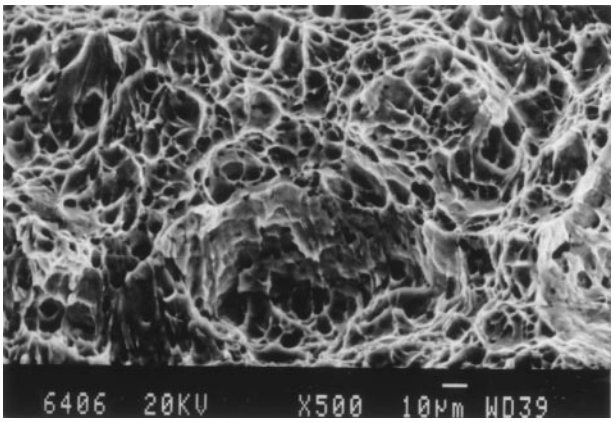

(*a*)

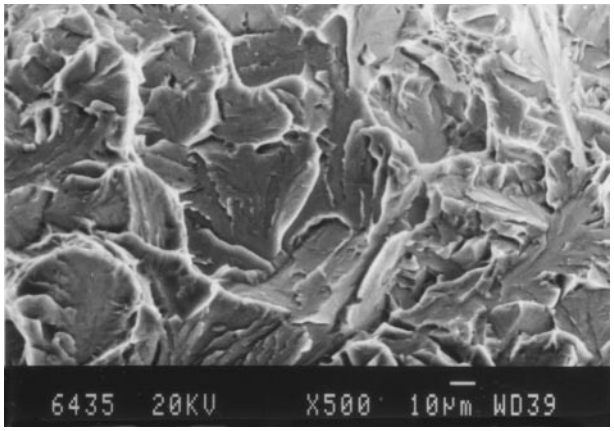

(*b*)

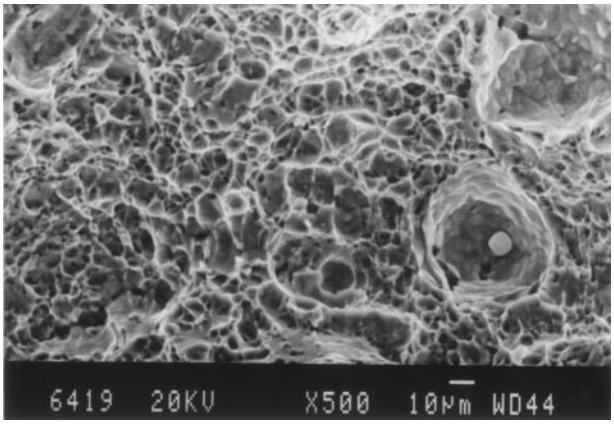

(*c*)

Fig. 10—SEM fractographs of the steel; charpy tested sample at −85 °C revealing (*a*) microvoids in as-quenched condition, (*b*) quasi-cleavage after 450 °C tempering, and (*c*) microvoids after 650 °C tempering.

IV. DISCUSSION

A. *Microstructure*

1. *As-quenched steel*

The microstructure of the water-quenched steel was martensitic, as shown by light microscopy (Figure 1) as well as by TEM (Figure 2(a)). Though the incidence of a small percentage of retained austenite at lath boundaries in quenched HSLA-100 steel was reported by earlier researchers,[15,16] the researchers did not support this by either XRD or SAD. Even in the present investigation, it was difficult to obtain SAD patterns for retained austenite in the quenched steel (Figure 2(e)), as the volume percent of retained austenite was very small and appeared in traces at a few lath boundaries, contrary to the amount shown by Mujahid *et al.*[16]

The existence of Nb(C, N) precipitates in the quenched structure may be expected because these might have formed during the hot-rolling process and did not go into solution at the austenitizing temperature. Cooke *et al.*,[18] in their work on HSLA-100 steel, proposed precipitation of that Nb(C, N) during the hot-rolling process. However, Fox *et al.*[15] and Foley and Fine[17,19] found the existence of fine spherical precipitates of Fe_3C in the quenched steel, although no diffraction evidence was provided. The occurrence of Cu precipitates in the quenched steel of the present investigation was, however, unusual, as no previous researcher had reported this. This phenomenon has probably occurred as a result of the higher copper content (~1.77 wt pct) of the present steel.

2. *Steel tempered at 450 °C*

Although coherent and incoherent precipitation of Cu was reported by earlier researchers,[15,16] the profuseness of the precipitation of Cu, to the extent of that observed by the present investigators at 450 °C tempering, was not reported before. As higher Cu content (1.77 wt pct) in the steel under investigation could be the reason that the heavily supersaturated α-iron matrix with Cu on quenching resulted in the profuse precipitation of Cu on tempering, even at a lower temperature. Mujahid *et al.*[16] observed the presence of fine copper clusters manifested by Moiré patterns when the steel was tempered at 450 °C. Their observations of spherical Nb(C, N) precipitates, 10 to 30 nm in diameter, support our observation. In contrast, Fox *et al.*[15] found very fine spherical particles, 5 to 10 nm in diameter, which they thought were a M_3C type of carbides, although they could not obtain any EDS spectrum or diffraction pattern from the carbides in support of their observations. Fox *et al.*[15] could not image Cu precipitates on tempering at 450 °C and concluded that all Cu precipitates must be the coherent type.

3. *Steel tempered at 650 °C*

The large number of Cu precipitates observed after tempering at temperatures up to 600 °C were, by and large, spherical (Figure 4). However, on tempering at 650 °C, the Cu precipitates become elongated and were rod-shaped. A new dark phase, which was established by TEM to be martensite or acicular ferrite, appeared along the lath boundaries. Mujahid *et al.*[16] has also observed this lath boundary dark phase. According to them, the new austenite formed on tempering above 665 °C transformed to martensite on subsequent air cooling to room temperature, and left behind substantial amounts of retained austenite, which appeared as a dark phase at the lath boundaries. However, our investigation reveals that this lath boundary dark phase (Figure 5(a)) is either martensite or acicular ferrite, which could be freshly formed from intercritical austenite on cooling. This is supported by the fact that the present investigation did not reveal any austenite peak in XRD. However, a very small amount of retained austenite could pre-exist in the structure from the as-quenched state and, since its amount was very small

(and could be detected as extremely fine films along the lath boundaries, as seen by TEM and not detected by XRD), it was not expected to have any effect on the steel's mechanical properties.

4. *Steel tempered at 700 °C*

The steel tempered at 700 °C exhibited a greater volume percentage of new dark phase (martensite); this was expected, since the temperature range was above the austenite forming critical temperature (AC_1) and more austenite phase was expected to form. The austenite formed above the AC_1 temperature transformed to martensite on rapid cooling in water to room temperature. The intercritical austenite formed at 700 °C was also expected to be rich in alloying elements, which would cause depletion of the alloying elements in the adjacent matrix. The latter observation has been confirmed by EDS microanalyses.

B. *Mechanical Properties*

The changes in the mechanical properties of the experimental steel on tempering could be divided into several stages. In stage I, from room temperature (25 °C) to 350 °C, the YS, UTS, and hardness remained more or less the same as that of the quenched steel. A small decrease of 30 MPa in UTS and a decrease in hardness of 11 VHN with an insignificant change in YS were, however, noticed on tempering at 350 °C. This small dip in UTS and hardness at this early stage is commonly observed during the tempering of quenched steel. Because of this particular trend of lowering of UTS and hardness at the early stage, the heat treatment of this steel after quenching can probably be better termed as "tempering" than "aging" (the latter term having been used by many previous researchers). In an aging process, one would expect a continuous increase in strength and hardness similar to that in any of the age-hardening alloys. Takashi Abe *et al.*[10] had observed a similar trend of decreasing strength at 450 °C while studying the aging behavior of a thermomechanically processed ASTM A 710 grade of steel. The tempering behavior of HSLA-100 steel in this temperature range (300 °C to 350 °C), however, has not been studied so far; it is being reported here for the first time. Figures 11(a) through (c) depict the YS, UTS, and VHN, respectively, *vs* the tempering temperature plots of HSLA-100 steel investigated by earlier workers, superimposed with the plots of the present authors. Wilson *et al.*[3] also showed that there was a slight decrease in the UTS of HSLA-100 or HSLA-80 steel on tempering at 400 °C, without any decrease in the YS.

Hardness and strength increased on tempering in the range of 350 °C to 450 °C (this may be called stage II) and reached a peak at 450 °C. The increments of the increase in YS, UTS, and VHN that resulted from increasing the tempering temperature from 350 °C to 450 °C were 180 and 114 MPa, and 42 VHN, respectively. The fine precipitates of Cu found in large quantities (Figure 3) are expected to hinder the dislocation movement; this results in a considerable rise in strength and hardness. Similar increases in the strength and hardness of HSLA-100 steel in this temperature range were also observed by earlier researchers.[3,15,16] Mujahid *et al.*[16] and Fox *et al.*[15] have all attributed this rise in strength to the formation of coherent Cu precipitates at this temperature. Fox *et al.* had also discussed the possible role of incoherent Cu precipitates in this strength increment. Goodman *et al.*,[20] Othen *et al.*,[21] and Le May and Krishnadev[22] considered the role of incoherent Cu precipitates in the rise of strength on tempering; this agrees with the findings of the present work. For HSLA-80 steel, Wilson *et al.*[3] has observed the peak strengthening at 510 °C.

A continuous decrease in strength and hardness develops in the temperature range 450 °C to 650 °C (stage III), and reaches minimum for 650 °C tempering. The softening of the matrix on tempering and the coarsening of Cu precipitates (Figure 5(b)) lowered the stress for the movement of dislocations at this stage, and resulted in a decrease in strength and hardness. The fresh martensite formed in the later part of stage III, at 650 °C, had no obvious significant effect on the strength properties due to its small percentage. The YS, UTS, and hardness were reduced by 335 and 281 MPa, and 99 VHN, respectively, from 450 °C to 650 °C. Earlier researchers[3,15,16] also observed similar decreases in strength in this temperature range (Figures 11(a) through (c)). Fox *et al.*[15] attributed this decrease in strength to the loss of coherency and coarsening of Cu precipitates. Mujahid *et al.*[16] have attributed the decrease in strength to the loss of coherency of Cu precipitates and the beginning of recovery and recrystallization processes in the matrix. Although partial recovery of the lath structure was noticed at 650 °C in the present work, there was no evidence of recrystallization of the matrix. Studies of other Cu-precipitation-hardening steels, HSLA-80 and ASTM A 710 steel, by Wilson *et al.*[3] and Hicho *et al.*,[8,9] respectively, have also indicated similar decreases in strength properties in this temperature range; this is attributed to the recovery of the lath matrix structure and the coarsening of the copper precipitates.

In stage IV of tempering, from 650 °C to 700 °C, the UTS and hardness increased slightly by 103 MPa and 20 VHN, respectively. These increases are attributed to the formation of alloy-rich fresh martensite in a larger quantity (Figure 6(a)) from the intercritical austenite phase upon quenching. The YS, however, experienced a declining trend in this stage due to considerable softening of the tempered lath martensite structure, which involved a drastic decrease in the dislocation density. There has, however, been an increase in UTS, which can be attributed to the substantial quantity of fresh martensite formed on cooling from 700 °C. The formation of fresh martensite increases the dislocation density in the surrounding ferrite, which lowers the yield strength but increases the UTS through higher strain hardening. Foley and Fine[17] also observed a decrease in YS and an increase in UTS on tempering at 700 °C. Mujahid *et al.*[16] also showed a rise in UTS and hardness in this temperature zone (Figures 11(b) and (c)), but they observed a rise in YS as well (Figure 11(a)), which is in contrast to our observation.

The EL percent of the steel remained more or less the same (~17) for tempering at temperatures up to 450 °C. In stage III (450 °C to 650 °C), there was little improvement in EL percent, and it reached a maximum of 23 after tempering at 650 °C. From the superimposed plots of EL *vs* tempering temperature shown in Figure 11(d), it can be seen that other researchers[16,23] have also obtained similar increases in EL in this temperature range. In stage IV of tempering (650 °C to 700 °C), deterioration of EL was noticed again; it was lowered to 18 pct after tempering at 700 °C. The

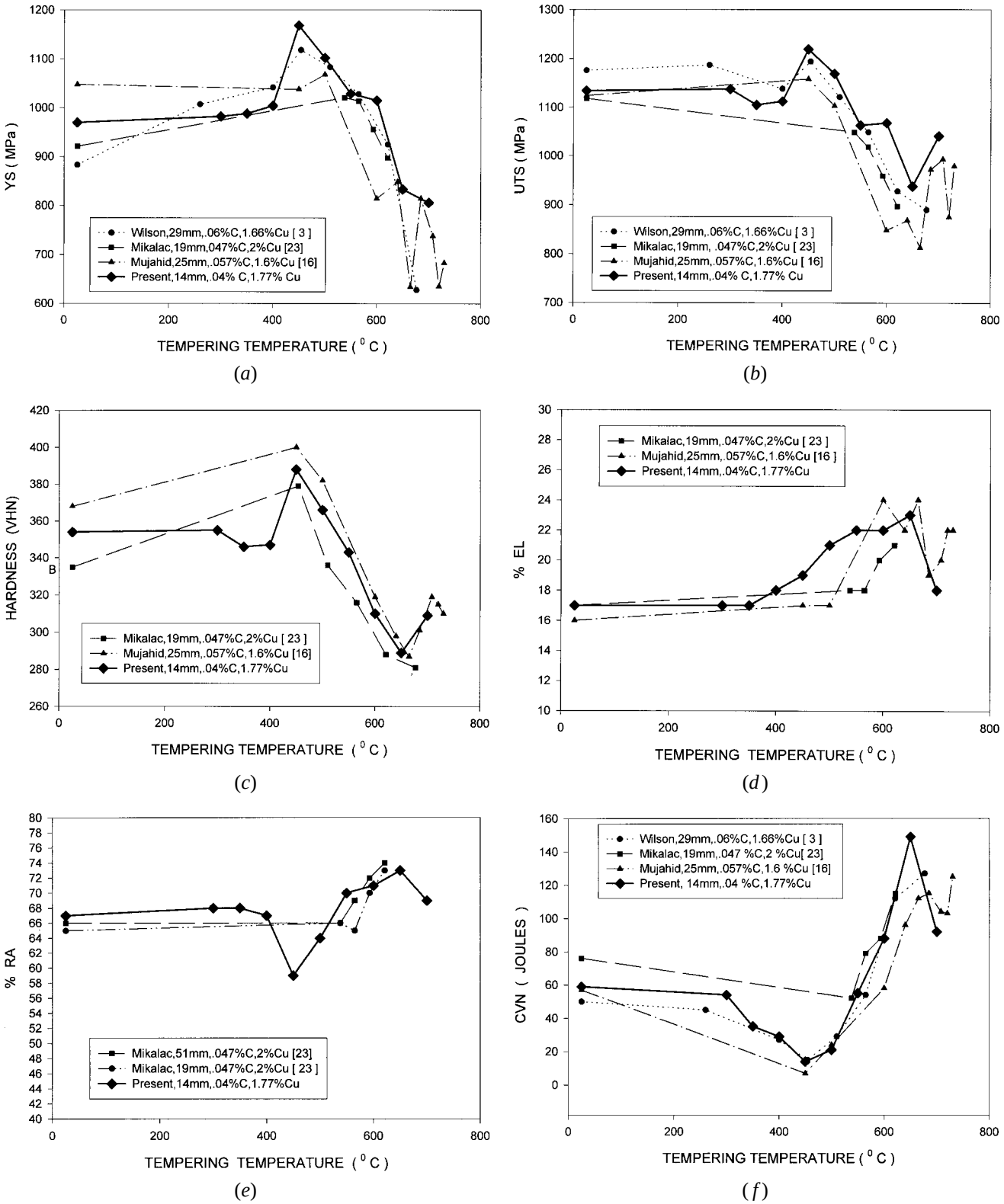

Fig. 11—Superimposed plots depicting variation of (*a*) YS, (*b*) UTS, (*c*) VHN, (*d*) EL percent, (*e*) RA percent, and (*f*) CVN at −85 °C with tempering temperature of the present investigation along with those of earlier workers.

present findings support the earlier observations of Mujahid *et al.*[16]

After remaining more or less constant in stage I, the RA percent of this steel was lowered to 59 at 450 °C from 67 at 350 °C in stage II of tempering. In stage III, there was continuous improvement in RA and it reached a maximum of 73 pct at 650 °C tempering temperature. Mikalac and Vassilaros[23] have also observed a similar rise in the RA percent in the temperature range, as can be seen from the superimposed plots shown in Figure 11(e). Hicho *et al.*[8]

also found a continuous improvement of the RA percent in this temperature range for the ASTM A 710 grade of steel. In stage IV of tempering, the RA percent went down slightly to 69 at 700 °C.

From the pattern of changes in the EL and RA percents with tempering temperature, it could be understood that the decrease in ductility in the lower temperature range near 450 °C is due to peak strengthening of the matrix, whereas in the higher temperature range (500 °C to 650 °C), the softening of the matrix on tempering has resulted in achieving a higher EL and RA percent. The decline in the values of the EL and RA percent after tempering at 700 °C could be attributed to the freshly formed hard martensite.

The Charpy impact toughness of the steel showed a little improvement at the beginning of stage I of tempering (25 °C to 350 °C), both for room temperature and at −20 °C test temperatures. The CVN at −85 °C, however, remained more or less the same, at ~60 J. The CVN values at all test temperatures, however, went down thereafter, reaching a minimum at 450 °C. The strengthened matrix is obviously detrimental for notch toughness. Mujahid *et al.*[16] and Wilson *et al.*[3] also observed similar dips in CVN values at the 450 °C tempering temperature, which could be seen in the superimposed plots of CVN at −85 °C *vs* tempering temperature (Figure 11(f)). Mujahid *et al.*[16] has attributed this to both the negative effect of matrix strengthening and the impurity segregation at the grain boundaries. But, since the fractographic studies of impact-tested samples at −85 °C revealed that the fracture of the 450 °C tempered steel was essentially a transgranular quasi-cleavage mode, the role of grain boundary impurities in bringing down the notch toughness has to be ruled out. A similar decrease in CVN values for HSLA-80 steel in the temperature range from 260 °C to 510 °C was also reported earlier.[3]

In stage III of tempering (450 °C to 650 °C), there was a remarkable improvement in CVN, reaching a peak at 650 °C. The impact toughness at −85 °C improved by 135 J on tempering at 650 °C, compared to that at 450 °C. The phenomenal improvement in impact toughness in this temperature range is due to the overaged microstructure of partially recovered matrix and coarse Cu precipitates, which might have helped in arresting the propagation of cleavage cracks. The increase of the EL and RA percent at this phase, as discussed earlier, matched the rise in CVN values. Mujahid *et al.*[16] has attributed this extraordinary improvement in toughness to the formation of highly alloyed, thermally stable austenite at the lath boundaries. As discussed previously (Section 4.2 of the referred paper (Ref. 16)), the present authors could find only traces of retained austenite at the lath boundaries and, hence, considered it not to be responsible for improved toughness. The phenomenal rise in toughness in other Cu-bearing low-alloy steels, the HSLA-80 and the ASTM A 710, was also reported by Wilson *et al.*[3] and Hicho *et al.*[8] in this temperature range.

In stage IV of tempering (650 °C to 700 °C), a slight decrease in CVN value was noticed after tempering at 700 °C. The higher volume percent of the freshly formed hard martensite on tempering at this temperature results in a loss of toughness. Mujahid *et al.*[16] and Foley and Fine[18] also observed lowering of the CVN at this phase.

Thus, in the present study, it has been found that the Cu precipitates and the newly formed martensite played a significant role in influencing the tempering behavior of the steel. The Nb(C, N) particles, which have been inherited in the quenched steel and exist in all tempered conditions, however, do not have any significant effect on the steel's tempering characteristics. A study of the mechanical property data revealed that the peak strength and toughness of the steel are obtained, after tempering at 450 °C and 650 °C, respectively, with their best combination achieved after tempering at 600 °C.

V. CONCLUSIONS

1. The water-quenched microstructure of the HSLA-100 steel plate (14-mm thick) was mostly lath martensite. Traces of retained austenite could be located at a few lath boundaries. Incidences of Cu and Nb(C, N) precipitates were observed in the quenched structure. A profuse precipitation of Cu as fine spherical particles was noticed at or above 450 °C, and coarsened to elongated rods at 650 °C. The steel was found to be highly resistant to tempering, and the martensite lath structure was visible even after tempering near intercritical temperature.
2. The YS and UTS of the steel varied in the ranges of 806 to 1168 MPa and 938 to 1219 MPa, respectively. Both YS and UTS were at their highest at 450 °C, and dropped down to their lowest at 700 °C and 650 °C tempering temperatures, respectively. The hardness of the steel was within a range of 289 to 366 VHN and, as expected, followed the same trend as UTS on tempering.
3. The EL percent was more or less constant at about 17 up to 450 °C tempering, beyond which it increased gradually to 23 on tempering at 650 °C. The RA percent also remained unchanged (~66) up to 350 °C, but experienced a fall on 450 °C tempering, to give the minimum value of 59, above which it started rising again and registered a maximum (~73) on 650 °C tempering.
4. The CVN impact toughness of the steel was lowest at 450 °C and highest at 650 °C tempering temperatures. At −85 °C, it registered 14, 149, and 92 J, after tempering at 450 °C, 650 °C, and 700 °C, respectively. While the profuse precipitation of Cu is considered responsible for the drastic fall in impact toughness on 450 °C tempering, the phenomenal rise in toughness at 650 °C is associated with the recovery of martensite laths and the coarsening of Cu precipitates. The decrease in toughness on tempering at 700 °C is attributed to freshly formed martensite.
5. The best combination of strength and toughness for the steel is obtained on tempering at 600 °C for 1 hour (YS-1015 MPa, UTS-1068 MPa, and CVN-88 J at −85 °C).

ACKNOWLEDGMENTS

The authors acknowledge the financial assistance provided through an INDO-US Project coordinated by the United States Naval Research Laboratory and the National Metallurgical Laboratory (Jamshedpur, India). Thanks are also expressed to the management of the R&D Centre, Steel Authority of India Limited (Ranchi), and the Head of the Department of Metallurgical Engineering, Banaras Hindu University (Varanasi), for providing the necessary experimental facilities.

REFERENCES

1. E.J. Czyryca: *Key Engineering Materials*, Trans Tech Publications, Aedermannsdorf, Switzerland, 1993, vols. 84–85, pp. 491-520.
2. B.A. Graville: *Proc. Int. Conf. on Welding of HSLA (Microalloyed) Structural Steels*, ASM INTERNATIONAL, Metals Park, OH, 1978, pp. 85-101.
3. A.D. Wilson, E.G. Hamburg, D.J. Colvin, S.W. Thompson, and G. Krauss: *Proc. Int. Conf. on Microalloyed HSLA Steel, Microalloying'88*, ASM INTERNATIONAL, Metals Park, OH, 1988, pp. 259-75.
4. A.K. Lis, M. Mujahid, C.I. Garcia, and A.J. DeArdo: *Speich Symp. Proc.*, ISS, Warrendale, PA, 1992, pp. 129-38.
5. R.H. Philips, J.G. Williams, and J.E. Croll: *Proc. Int. Conf. on Microalloyed HSLA Steels, Microalloying'88*, ASM INTERNATIONAL, Metals Parrk, OH, 1988, pp. 235-47.
6. M.T. Miglin, J.P. Hirth, A.R. Rosenfield, and W.A.T. Clark: *Metall. Trans. A*, 1986, vol. 17A, pp. 791-98.
7. S.S. Banadkouki Ghasemi, D. Yu, and D.P. Dunne: *Iron Steel Inst. Jpn.* 1996, vol. 36, pp. 61-67.
8. G.E. Hicho, C.H. Brady, L.C. Smith, and R.J. Fields: *J. Heat Treating*, 1987, vol. 5, pp. 7-19.
9. G.E. Hicho, S. Singhal, L.C. Smith, and R.J. Fields: *Proc. Int. Conf. on HSLA Steels, Technology and Applications*, ASM INTERNATIONAL, Metals Park, OH, 1984, pp. 705-13.
10. Takashi Abe, Masayoshi Kurihara, and Histoshi Tagawa: *Trans. Iron Steel Inst. Jpn.*, 1987, vol. 27, pp. 478-84.
11. S.W. Thompson and G. Krauss: *Metall. Mater. Trans. A*, 1996, vol. 27A, pp. 1573-88.
12. A.D. Wilson: *J. Met.*, 1987, vol. 29, pp. 39-48.
13. S.W. Thompson, D.J. Colvin, and G. Krauss: *Metall. Mater. Trans. A*, 1990, vol. 21A, pp. 1493-1507.
14. S.W. Thompson, D.J. Colvin, and G. Krauss: *Metall. Mater. Trans. A*, 1996, vol. 27A, pp. 1554-68.
15. A.G. Fox, S. Mikalac, and M.G. Vassilaros: *Speich Symp. Proc.*, ISS, Warrendale, PA, 1992, pp. 155-61.
16. M. Mujahid, A.K. Lis, C.I. Garcia, and A.J. DeArdo: *J. Mater. Eng. Performance*, 1998, vol. 7, pp. 247-57.
17. R.P. Foley and M.E. Fine: *Proc. Int. Conf. on Processing, Microstructure and Properties of Microalloyed and Other Modern HSLA Steels*, ISS, Warrendale, PA, 1991, pp. 315-30.
18. M.A. Cooke, B.H. Chapman, and S.W. Thompson: *Scripta Metall.*, 1992, vol. 26, pp. 1553-58.
19. R.P. Foley and M.E. Fine: *Speich Symp. Proc.*, ISS, Warrendale, PA, 1992, pp. 139-54.
20. S.R. Goodman, S.S. Brenner, and J.R. Low: *Metall. Trans. A*, 1973, vol. 4, pp. 2363-78.
21. P.J. Othen, M.L. Jenkins, G.D.W. Smith, and W.J. Phythian: *Phil. Mag. Lett.*, 1991, vol. 64, pp. 383-91.
22. I. LeMay and M.R. Krishnadev: in *Copper in Iron and Steel*, I. LeMay and L.M. Schetky, eds., John Wiley and Sons, New York, NY, 1982, pp. 5-43.
23. S.J. Mikalac and M.G. Vassilaros: *Proc. Int. Conf. on Processing, Microstructure and Properties of Microalloyed and Other Modern HSLA Steels*, ISS, Warrendale, PA, 1991, pp. 331-43.